Acta Astronautica 220 (2024) 367–373

Contents lists available at ScienceDirect

Acta Astronautica

journal homepage: www.elsevier.com/locate/actaastro

Effects of UV-C exposure on composite materials made of recycled carbon fibers

Daniele Tortorici [a], Elisa Toto [a,b], Maria Gabriella Santonicola [b], Susanna Laurenzi [a,*]

[a] Department of Astronautical Electrical and Energy Engineering, Sapienza University of Rome, Via Salaria 851-881, 00138 Rome, Italy
[b] Department of Chemical Engineering Materials Environment, Sapienza University of Rome, Via del Castro Laurenziano 7, 00161 Rome, Italy

ARTICLE INFO

Keywords:
Composite material
recycled carbon fiber
UV-C radiation
Space sustainability

ABSTRACT

Carbon fiber-reinforced polymers are widely used in space applications since they combine outstanding mechanical properties with low material density. However, the development of composite components involves raw materials that are becoming increasingly scarce and contributes significantly to carbon emissions during the manufacturing process. Indeed, the fabrication of fibers is energy-intensive and requires very high temperatures, high costs, and usually precursor materials derived from fossil fuels. In addition to the negative environmental impact due to the manufacturing process, there are critical issues related to the disposal of components fabricated using carbon/glass fiber composites. Therefore, the use of efficient recycling strategies becomes necessary, according to economic reasons and legislation. The recycled fibers exhibit different properties from virgin fibers, generally lower, due to adverse effects of the current recycling methods. In this study, we investigated the potential application of recovered carbon fibers in satellite platforms, using recycled fibers from our laboratory obtained with a subcritical solvolysis method that we have previously developed. Composite materials reinforced with recycled and virgin carbon fibers were exposed to UV-C, and the effects of irradiation were analyzed in terms of structural performance, surface morphology, and chemical modifications of the samples. Results were used to evaluate the possibility of effectively using recycled fibers in space applications, without significant loss of performance.

1. Introduction

Composite materials are widely used in space engineering since they can provide outstanding mechanical properties by combining a suitable matrix with fiber reinforcement [1–3]. Carbon fiber (CF) is the material of choice when high modulus or high strength is required, as in the case of structural components [4]. Composite structures offer significant weight saving when is used to replace metallic counterparts in the automotive and aeronautic industries, thereby providing a positive environmental impact [1,2]. Indeed, utilizing composite structures leads to reduce mass to meet the structural requirements with a consequent decrease in fuel consumption over the service life [4,5]. In space applications, the weight saving immediately results in costs reduction for the launch phase.

However, the fabrication of composite materials involves a high amount of energy and precursor materials derived from fossil fuels. Several authors evaluated the amount of energy related to the production phase of fibers ranging from tens of MJ/kg for glass fibers to hundreds of MJ/kg for CFs [6–8]. Furthermore, CFs are produced from fossil fuel-derived precursors such as polyacrylonitrile and mesophase pitch with a huge environmental impact [9]. In addition, composites that reach the end of life are treated as hazardous waste and are typically disposed of in landfills [10].

The heterogeneity of composite materials makes the recycling process complex, where different approaches are applicable to materials with distinct properties. Common methods for composite recycling encompass mechanical, thermal, and chemical-based treatments [11–13]. Recycling efforts can aim at recovering all constituents or focus only on the reinforcing fibers. Our previous investigation adopted the latter approach to reclaim carbon fibers from epoxy-based composites [14]. The recycled fibers exhibited no significant chemical or surface topographical degradation. Although there was a 9 % reduction in

Abbreviations: Carbon fiber, (CF); recycled carbon fibers, (rCFs); virgin carbon fibers, (vCFs); low Earth orbit, (LEO); ultraviolet, (UV); Fourier transform infrared spectroscopy, (FTIR); Scanning electron microscopy, (SEM).

* Corresponding author.
E-mail address: susanna.laurenzi@uniroma1.it (S. Laurenzi).

https://doi.org/10.1016/j.actaastro.2024.05.004
Received 15 January 2024; Received in revised form 24 April 2024; Accepted 3 May 2024
Available online 4 May 2024

elastic modulus due to the process, and the chemical treatment resulted in sizing removal, impacting adhesion at the fibers/matrix interface [15], it does not hinder the reusability of these fibers. This is a key aspect to be pointed out and can significantly boost the industry and user's confidence, facilitating the widespread adoption of composite recycling. In this study, we inquire about the possibility to use recycled carbon fibers (rCFs) to fabricate composite materials tailored for space applications. Composite materials play crucial roles in various components of spacecraft, including strap elements, booms, housings, solar panels, and satellite antennas [16,17]. Surprisingly, despite the widespread use of composites in space applications, no prior research has explored the use of rCFs in this context. The novelty of our study lies in addressing this gap by evaluating the suitability of such fibers for these demanding applications in space.

The fibers used in this study are coming from the previously developed recovery process and were employed for the fabrication of composites subjected to testing under space environment conditions. Focusing on low Earth orbit (LEO), one of the primary sources of degradation for composites is the ultraviolet (UV) radiation, emitted by the sun and falling within the wavelength range of 100–400 nm [18]. UV-C radiation (wavelength range 100–280 nm) poses the most significant threat, as its energy, inversely proportional to the wavelength, is sufficient to break the C–C and C–O bonds of polymers and their functional groups [19]. In this study, the effects of UV-C irradiation on CF/epoxy composites, made of recycled carbon fibers, were investigated. Samples were exposed to a 1-year LEO equivalent dose of UV-C irradiation and its effects were evaluated using different experimental techniques. Dynamical mechanical analyses were performed to evaluate any post-irradiation modulus drop and to examine the influence of recycled and virgin fibers on the mechanical behavior of the samples. The chemical composition of the composites was investigated by Fourier transform infrared spectroscopy (FTIR). Spectra of both unirradiated and irradiated composites were compared to assess the impact of different fiber types (rCFs/epoxy and virgin CFs/epoxy), before and after UV-C exposure. Additionally, the surfaces of the specimens were analyzed by scanning electron microscope (SEM) to identify defects both before irradiation and UV-C-induced damage. The comprehensive results obtained provide invaluable insights into the impact of employing recycled fibers on composite properties and their behavior under UV-C radiation, as encountered in Low Earth Orbit (LEO).

2. Material and methods

2.1. Samples fabrication

Composites were fabricated using Tenax-E IMS65 E23 carbon fiber yarns from Teijin (Tokyo, Japan). These are high-performance carbon fibers largely used in the aerospace industry. They are supplied with an epoxy sizing compatible with thermoset matrix systems. The characteristics of the carbon fiber were listed in Table 1.

Concerning the matrix, we used the epoxy resin PRIME 20LV from Gurit (Wattwil, Switzerland). The slow hardener was used with the mix ratio by weight of 26:100 with respect to the resin. The cure scheme followed was 7 h at a temperature of 65 °C, according to the resin datasheet. Despite its low glass transition temperature, which may not be optimal for space applications, this resin was chosen for the initial study due to its advantageous properties, including low viscosity, extended working time, and minimal thermal curing requirements. Twenty samples, each measuring 40 × 5 × 0.75 mm nominally, were produced for the study. Seven layers of yarn were employed, achieving a fiber volume fraction of around 14 %. The fibers were aligned parallel to the major dimensions of the specimens. Ten specimens were fabricated using virgin carbon fibers (vCFs), while the remaining ten utilized recycled carbon fibers (rCFs) sourced from a previously established solvolysis-based process [14]. In particular, a solution of sulfuric acid and demineralized water was used to selectively degrade the polymeric matrix of the vCFs/Epoxy composites, resulting in fibers without significant damage. Recycled fibers were washed with demineralized water and acetone before being dried and preparing for reusing.

Table 1
Characteristics of Tenax-E IMS65 E23 carbon fiber.

Diameter	5 μm
Elastic modulus	290 GPa
Tensile stress	6000 MPa
Sizing type	Epoxy
Precursor	Poly-acrylonitrile (PAN)

2.2. UV-C irradiation

vCFs/Epoxy and rCFs/Epoxy composite samples (five replicates) were exposed to UV-C radiation. Irradiation was performed using a low-pressure UV lamp (3UV-38, 8 W from UVP LLC, USA [20]) at a wavelength of 254 nm. Irradiation was carried out in a closed chamber coated with aluminum foil, with a source-samples distance of 85 mm (Fig. 1) [21]. The UV-C intensity was set to 1 mW/cm^2 and measured with an HD 2302.0 photo-radiometer equipped with an LP 471 UV-C probe (spectral range 200–280 nm). Samples were exposed to UV-C for about 8 days in order to achieve a total dose of 716 J/cm^2, which corresponds to the dose experienced in a 1-year period in LEO, according to the average radiation measured intensity of $2.27 \cdot 10^{-2}$ mW/cm^2 [22].

2.3. Characterization methods

The elastic storage modulus (E') and the damping factor (tanδ) were measured using the dynamical mechanical analyzer DMA-1 (Mettler Toledo, Greifensee, Switzerland). Tests were performed in dual cantilever mode, with a length of 25 mm, a frequency of 1 Hz and a displacement amplitude of 10 μm. Measurements were carried out in the temperature range from 30 °C to 100 °C, with a rate of 3 °C/min. Three specimens for type were tested to ensure reproducibility of results.

The chemical structure of samples was investigated by Fourier transform infrared spectroscopy using a Nicolet Summit FTIR Spectrometer (Thermo Fisher Scientific, Waltham, MA, USA) in attenuated total reflectance mode. Spectra were acquired in the wavenumber range 500–4000 cm^{-1}, at a spectral resolution of 4 cm^{-1}, averaging 64 scans per measurement. Absorption peaks of the materials before and after irradiation were identified and relevant chemical bonds assigned to evaluate the chemical modification induced by UV-C exposure.

The morphology of the composites was investigated before and after UV-C exposure using a VEGA II LSH scanning electron microscope (TESCAN, Brno, Czech Republic), with an accelerating voltage of 20 kV and a magnification of 1000 × . A sputter coater (Cressington 108auto) was used to create a thin metal film in order to observe the non-conductive surface of the specimens. For each sample, six images were acquired and analyzed to assess the changes induced by radiation. Image processing was performed with an algorithm implemented in MATLAB: for each image, a threshold was identified in order to make a conversion from the greyscale to a binary image (black and white pixels). Then, white pixels, which represent defects [23], were summed and their percentage with respect to the total evaluated, allowing a direct comparison of the different images.

3. Results

3.1. Mechanical characterization

Fig. 2 shows the measured elastic storage modulus (E') of unirradiated and irradiated specimens for both vCFs/Epoxy and rCFs/Epoxy at the starting temperature (30 °C). For the unirradiated rCFs/Epoxy samples, E' was found to be about 20.2 % lower than the value measured

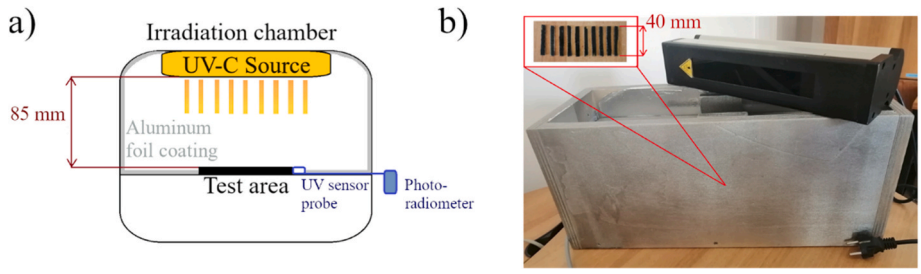

Fig. 1. a) schematic representation of the experimental setup illustrating the configuration and relevant dimensions involved in the UV-C irradiation process; b) experimental setup is depicted, showcasing how the setup is configured in practice.

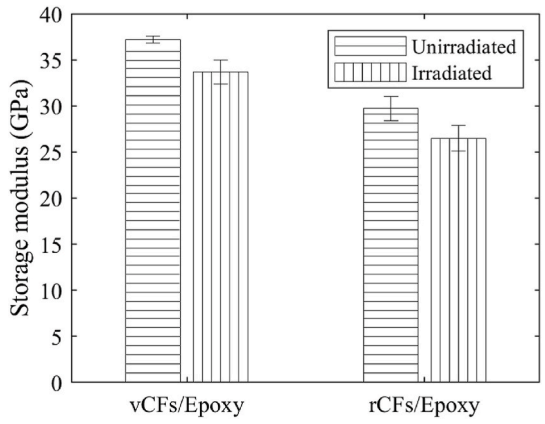

Fig. 2. Measured values of E' at 30 °C for vCFs/Epoxy and rCFs/Epoxy specimens in the unirradiated and irradiated case.

for the vCFs/Epoxy samples (29.7 ± 1.3 GPa versus 37.2 ± 0.4 GPa). After UV-C exposure, this difference increases to 21.4 %. In fact, E' decreases by 9.5 % (33.7 ± 1.3 GPa versus 37.2 ± 0.4 GPa) for vCFs/Epoxy specimens and by 10.8 % (26.5 ± 1.4 GPa versus 29.7 ± 1.3 GPa) for rCFs/Epoxy composites.

Fig. 3 depicts E' as a function of temperature for vCFs/Epoxy (Fig. 3a) and rCFs/Epoxy specimens (Fig. 3b). At the initial test temperature of 30 °C, we observe the aforementioned decrease in moduli, which continues consistently with increasing temperature until the composites undergo a decline in modulus due to matrix softening, signaling the initiation of the glass transition [24]. Post-irradiation, this transition occurs at a higher temperature for both types of composites, attributed to further resin curing prompted by UV-C exposure [25,26]. In particular, we found an onset temperature of about 67.7 ± 1.2 °C for unirradiated vCFs/Epoxy, 77.6 ± 0.6 °C for irradiated vCFs/Epoxy, 65.3 ± 1.2 °C for unirradiated, and 77.8 ± 1.5 °C for irradiated rCFs/Epoxy. Looking at the damping factor, a shift of the curve towards higher temperature can be detected after the UV-C exposure (Fig. 4). In particular, the unirradiated composites made with vCFs show a peak at 83.0 ± 1.0 °C, whereas for the irradiated samples the peak shifts at 93.3 ± 1.5 °C (~+10 °C) (Fig. 4a). Similarly, for the composites with rCFs, the damping factor peak shifted from 81.3 ± 1.2 °C to 95.7 ± 1.2 °C (~+15 °C) (Fig. 4b).

3.2. Chemical characterization

FTIR spectrum of the unirradiated neat epoxy was acquired after the curing process (Fig. 5) and compared with that of unirradiated and irradiated composites fabricated using vCFs (Fig. 5a) and rCFs (Fig. 5b). The following absorption bands were observed for the neat epoxy: 3387, 3035, 2958, 2922, 2853, 1740, 1607, 1582, 1508, 1456, 1382, 1240, 1181, 1105, 1031, 932, and 825 cm^{-1}. The band-assignments were listed in Table 2.

3.3. Morphological characterization

The surface of specimens appears smooth and uniform to the naked eye before irradiation. However, following SEM analysis conducted at a magnification of 1000 × , some defects become visible (Fig. 6). In both vCFs/Epoxy (Fig. 6a) and rCFs/Epoxy (Fig. 6b) composites, these defects exhibit a maximum size of 25 μm and are evenly distributed across the surface.

Six images were acquired in different areas of each sample and analyzed by MATLAB. As defects and damages were discernible in lighter shades, the sample images underwent binarization, and the count of white pixels was recorded. The outcomes of this analysis are depicted in Fig. 7: the unirradiated surfaces exhibited a comparable percentage of white pixels (representing defects) in both rCFs/Epoxy and vCFs/Epoxy composites. Subsequent to irradiation, there was a noticeable increase in the percentage of white pixels in both cases, albeit more pronounced for

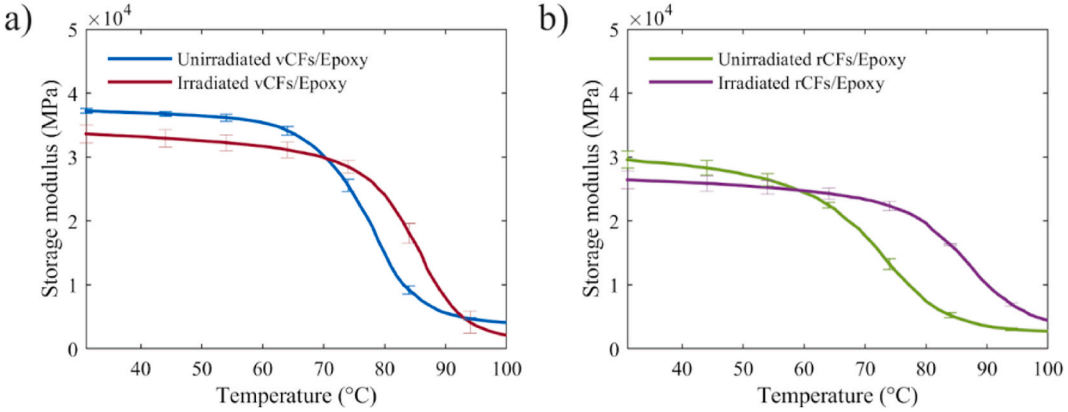

Fig. 3. Storage modulus as a function of temperature for: a) vCFs/Epoxy specimens; b) rCFs/Epoxy specimens.

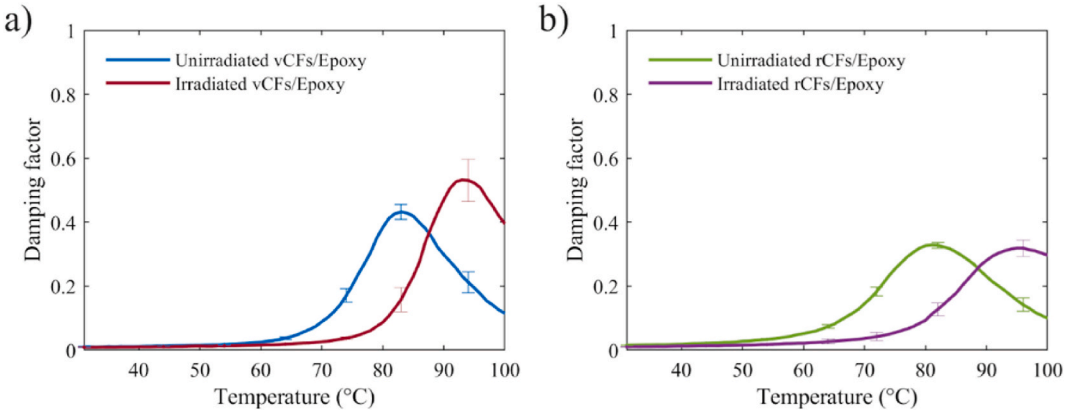

Fig. 4. Damping factor as a function of temperature for: a) vCFs/Epoxy specimens; b) rCFs/Epoxy specimens.

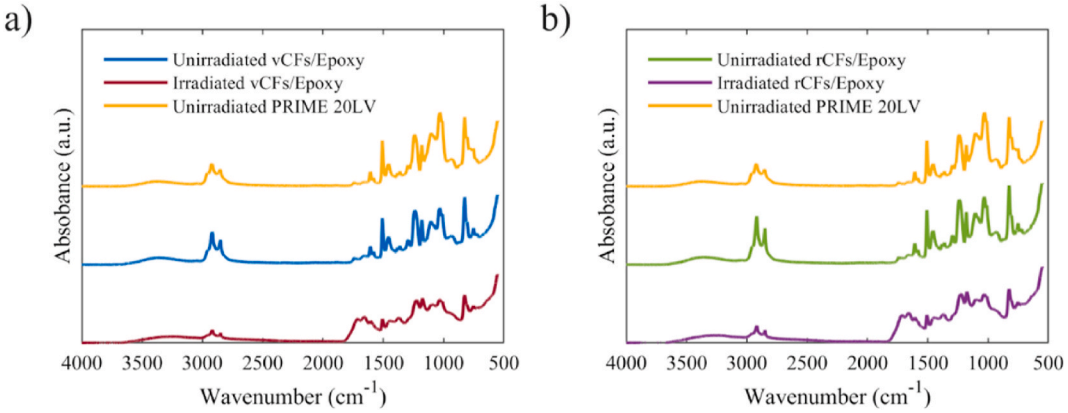

Fig. 5. ATR-FTIR spectra of unirradiated cured resin, a) vCFs/Epoxy specimens before and after exposure, and b) rCFs/Epoxy specimens before and after exposure. Data are offset for clarity.

Table 2
Assignments of the main absorption bands in the FTIR spectrum of unirradiated epoxy [27–29].

Wavenumber (cm^{-1})	Assignment
3387	O–H stretching
3035	C–H stretching
2958, 2922, 2853	C–H and $–CH_2$ stretching
1740	C═O stretching
1582, 1508, 1456	Aromatic ring stretching
1382	C–H deformation in aliphatic units
1240	C–O–C stretching of ether linkage
1181	Aromatic C–O stretching
1031	C–O–C stretching of ether linkage
932	Epoxy functional group
825	C–H deformation

the rCFs/epoxy composite (+243 % compared to +120 % for the vCFs/epoxy composite).

3.4. Discussion

The storage modulus of vCFs/Epoxy (Fig. 3a) and rCFs/Epoxy specimens (Fig. 3b) is reported as a function of temperature. Both materials exhibit a decrease in modulus, which continues consistently as the temperature rises until the composites undergo a decline in modulus due to the softening of the matrix, signaling the onset of the glass transition [24,30]. Post UV-C irradiation, this transition takes place at a higher temperature for both types of composites, attributed to further resin curing induced by UV-C exposure [25,26]. After exposure to a 1-year LEO equivalent dose of UV-C radiation, the storage modulus decreased by 9.5 % for vCFs-reinforced composites and by 10.8 % for rCFs-reinforced composites. Looking at the pre-irradiation values, the glass transition temperature remained largely unaffected by the type of fibers used. Post-irradiation, vCFs/Epoxy and rCFs/Epoxy materials exhibited the same glass transition temperature. The post-irradiation increases in Tg values observed in both types of composites, can be attributed to the effects of UV radiation: heightened degree of cross-linking in the polymer chain structure, the restriction of polymer chain mobility, and the formation of stronger bonds following exposure of thermosetting matrices to UV radiation. UV-C irradiation energy facilitates the formation of chemical bonds within the polymer chain of the matrix, thereby enhancing the cross-linking density and consequently raising the glass transition temperature. Indeed, during cross-linking reactions between the epoxy resin and the hardener, the C–O bonds of the epoxy groups are broken, causing the carbon end of the open epoxy group to react with the nitrogen atoms in the amine groups of the hardener [31,32]. Consequently, post-curing reactions occur after exposure to UV-C irradiation in incompletely polymerized materials. These results suggest that the use of rCFs had a negligible effect on the matrix crosslinking compared to vCFs.

The temperature associated with the peak of the damping factor mirrors the trend of the glass transition temperature. This peak denotes the maximum energy dissipation during the glass transition, marking the point at which the material absorbs the highest amount of energy and displays increased elasticity. Both materials exhibit a nearly identical temperature values associated with the peak, both before and after irradiation (Fig. 4). After exposure to UV-C radiation, there is an increase in temperature associated with the damping factor peak, which is

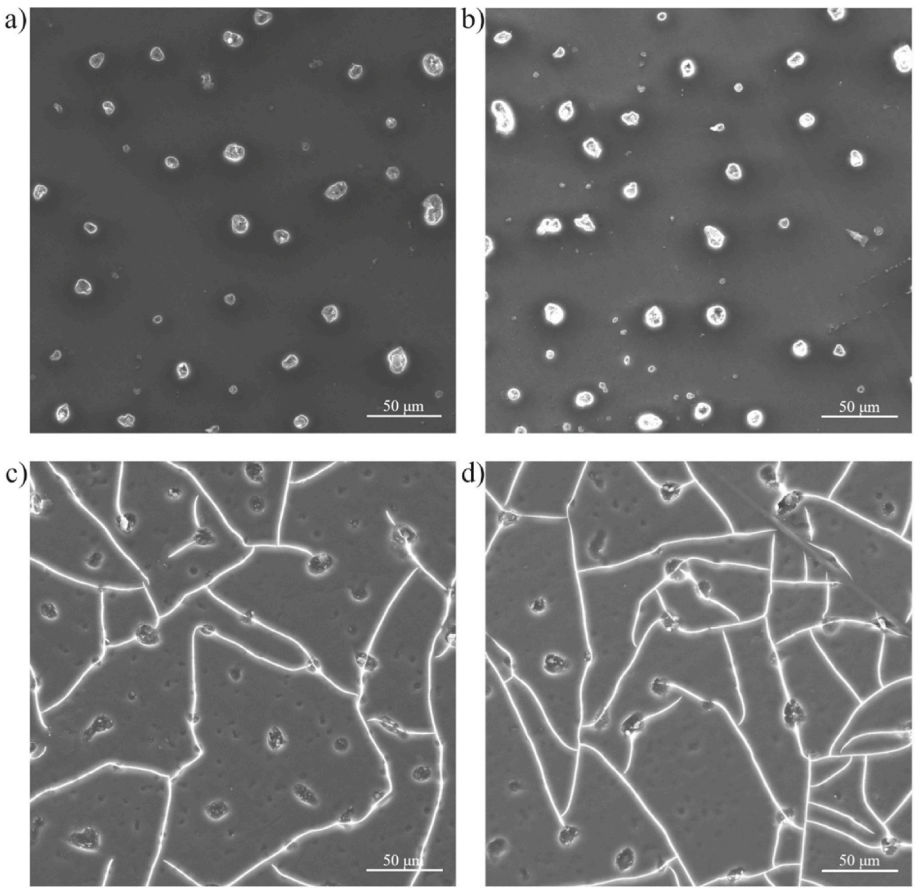

Fig. 6. SEM images of the surface of: a) vCFs/Epoxy unirradiated specimen; b) rCFs/Epoxy unirradiated specimen; c) vCFs/Epoxy specimen after UV-C exposure; d) rCFs/Epoxy specimen after UV-C exposure. Magnification: 1000 × .

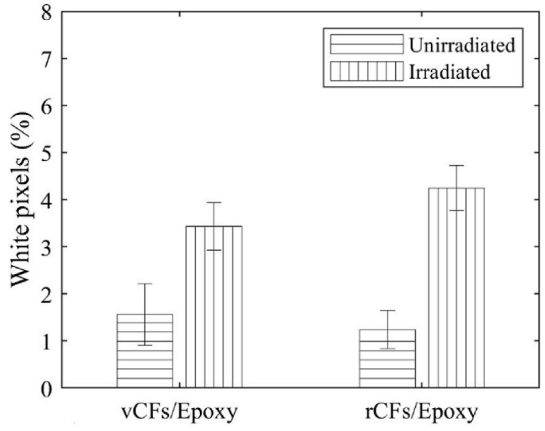

Fig. 7. Percentage of white pixels (defects) in SEM images of vCFs/Epoxy and rCFs/Epoxy specimens, in the unirradiated and irradiated case.

attributed to crosslinking phenomena resulting from irradiation exposure.

It's noteworthy that the damping factor in rCF/epoxy composites remains the same both before and after irradiation, whereas in vCF/epoxy composites, the damping factor increases. In addition, the damping factor of rCF/epoxy composites is lower than that of vCF/epoxy composites. These findings suggest that the bonding between the rCF and the epoxy matrix is stronger than that with vCF. Indeed, the primary source of damping in composites is the inherent damping of their constituents, with the viscoelasticity of the polymeric matrix being the main contributor. However, the interface between the matrix and fibers plays also a crucial role [33,34]. Several authors have established that the removal of sizing from fibers can enhance the interface bonding between matrix and fibers [35–38]. In our study, the elimination of the sizing is ensured through the solvolysis process [35], thereby resulting in a stronger modified bond between the matrix and rCF. Consequently, this leads to a reduction in the damping factor for rCF/Epoxy composites.

The morphological analysis shows that, after exposure to UV-C irradiation, the surfaces of both rCF-based and vCF-based composites exhibit signs of damage: cracks spanning the entire irradiated area become apparent, with these defects serving as nuclei for crack propagation (Fig. 6c and d). In particular, the more pronounced rise is observed for the rCFs/epoxy composite post-irradiation. These findings align with the occurrence of induced cross-linking reactions in the epoxy matrix upon exposure to UV C radiation. This results in a process referred to as post-curing, wherein the epoxy structure experiences heightened brittleness, ultimately leading to the emergence of micro-cracks within the epoxy framework [32,39]. The increased occurrence of defects in the irradiated samples provides justification for the decrease in storage modulus observed in both types of composites. This decrease can be attributed to a direct correlation between matrix cracking and the reduction in mechanical properties [40]. Moreover, in recycled carbon fiber (rCF)/epoxy composites, the fibers are not well-aligned in the longitudinal direction, unlike virgin carbon fiber (vCF)/epoxy composites, primarily due to the recycling process. This misalignment also results in a modification of the dynamic mechanical properties.

The ATR-FTIR analysis shows an increase in the absorption bands at 2958, 2922, 2853 cm^{-1} after adding CFs to the epoxy matrix. This

indicates C–H stretching vibrations of CH_3, CH_2, and CH groups derived from fibers, most marked when the recycled type was used [41]. After UV exposure, the peaks at 2958, 2922, 2853 cm^{-1} decrease in intensity, indicating that C–H bonds in methyl or methylene between two benzene rings were oxidized [27]. The epoxide unit band at 932 cm^{-1} appears negligible in the spectra of irradiated composites, unveiling that further curing took place in the matrix with reduction of epoxide unit and the formation of hydroxyl and carbonyl units [28]. The characteristic absorption peaks of the benzene ring near 1582, 1508 and 1456 cm^{-1} decreased in intensity, suggesting that the ring structure was altered by UV-C, and novel chemical species were formed [29]. The absorption bands of aromatic ether (1240 cm^{-1}), aliphatic ether (1105 cm^{-1}), C–O (1181 cm^{-1}) and C–H of substituted benzene (825 cm^{-1}) decreased, confirming that irradiation promotes oxidation, chain-break, and the generation of free reactive radicals both in the presence of recycled and virgin fibers [42]. Oxidation in low Earth orbit (LEO) can be significantly more pronounced compared to oxidation on Earth during the experiments, due to the abundance of atomic oxygen found between altitudes of 100 km and 650 km. Atomic oxygen originates from the photo-dissociation of molecular oxygen by solar vacuum ultraviolet light. Therefore, the density of atomic oxygen, and consequently the rate of erosion at a given altitude, is closely linked to solar activity [43,44].

Moreover, absorption bands at 1659 and 1712 cm^{-1} appeared in the spectra of irradiated samples, and this can be likely related to the UV-induced generation of photoproducts such as acetophenone (1659 cm-1) and benzyl methyl ketone (1712 cm-1) [28].

In summary, results indicate that the use of rCFs instead of vCFs in the manufacture of composites leads to a reduction in mechanical performance in terms of modulus and alters the load transfer capability at the fiber/matrix interface due to the removal of sizing caused by the recycling process. Nevertheless, sufficiently higher properties are retained. When composites are exposed to UV-C irradiation, they undergo physical and chemical damage. In addition, we observed a post-curing effect on the matrix promoted by UV-C irradiation. This would increase the matrix stiffness and thus the storage modulus of the composites. At the same time, irradiation caused the matrix cracking, with a negative effect on the modulus. Those phenomena cannot be seen separately from the current study and the results we observed are coupled. The same is true for the damping behavior which will be reduced by the post-curing and increased by the matrix cracking. Furthermore, we observed the oxidation of the specimen, which is expected to be more pronounced in low Earth orbit due to the high abundance of atomic oxygen species.

4. Conclusion

Recycled carbon fibers were utilized as reinforcement in the fabrication of epoxy-based composite materials, with their properties evaluated under UV-C exposure. Prior to UV irradiation, composites incorporating rCFs exhibited lower mechanical properties compared to those reinforced with virgin carbon fibers, a characteristic attributed to the chemical treatment undergone by the recycled fibers. Subsequent to exposure to a 1-year LEO equivalent dose of UV-C radiation, the storage modulus decreased by 9.5 % for vCFs-reinforced composites and by 10.8 % for rCFs-reinforced composites. A shift in the glass transition toward higher temperatures was observed for both composite types, indicating further resin curing induced by UV-C. This observation was corroborated by ATR-FTIR analysis. The resin selected for this study is the PRIME 20LV, characterized by a glass transition temperature below 100 °C. Consequently, it may not be the optimal resin for spacecraft applications, which often demand superior performance characteristics. Nevertheless, this study emphasizes the impact of utilizing rCFs instead of vCFs in composites exposed to the LEO radiation environment. The findings suggest that despite the resin's limitations, the use of rCFs has minimal detrimental effects on performance, thereby indicating their potential suitability for such applications.

In summary, the results indicate that UV-C exposure affects rCFs/Epoxy composites, yet they maintain functional properties that position them as promising candidates for space applications.

Data availability

The data that support the findings of this study are available on request to the corrisponding author.

CRediT authorship contribution statement

Daniele Tortorici: Data curation, Investigation, Validation, Writing – original draft. **Elisa Toto:** Validation, Writing – original draft. **Maria Gabriella Santonicola:** Methodology, Resources, Validation, Writing – review & editing. **Susanna Laurenzi:** Conceptualization, Funding acquisition, Investigation, Methodology, Supervision, Validation, Writing – review & editing.

Declaration of competing interest

The authors declare that they have no known competing financial interests or personal relationships that could have appeared to influence the work reported in this paper.

Acknowledgments

This work was financially supported by Sapienza University of Rome (Italy) (grant numbers MA21916B865F6B61, RM120172B73FC9DC).

References

[1] S. Laurenzi, A. Casini, D. Pocci, Design and fabrication of a helicopter unitized structure using resin transfer moulding, Compos. Appl. Sci. Manuf. 67 (2014) 221–232.
[2] S. Laurenzi, A. Grilli, M. Pinna, F. De Nicola, G. Cattaneo, M. Marchetti, Process simulation for a large composite aeronautic beam by resin transfer molding, Compos. B Eng. 57 (2014) 47–55.
[3] S. Laurenzi, D. Rufo, M. Sabatini, P. Gasbarri, G.B. Palmerini, Characterization of deployable ultrathin composite boom for microsatellites excited by attitude maneuvers, Compos. Struct. 220 (2019) 502–509.
[4] T.K. Das, P. Ghosh, N.C. Das, Preparation, development, outcomes, and application versatility of carbon fiber-based polymer composites: a review, Adv. Compos. Hybrid Mater. 2 (2019) 214–233.
[5] D. Tortorici, S. Laurenzi, M. Sabatini, L. Sorrentino, G. Parodo, S. Turchetta, High-performance thermoplastic composite structure for suborbital vehicles, in: Proceedings of the International Astronautical Congress, 2022. IAC.
[6] Y.S. Song, J.R. Youn, T.G. Gutowski, Life cycle energy analysis of fiber-reinforced composites, Compos. Appl. Sci. Manuf. 40 (2009) 1257–1265.
[7] T. Groetsch, M. Maghe, C. Creighton, R.J. Varley, Environmental, property and cost impact analysis of carbon fibre at increasing rates of production, J. Clean. Prod. 382 (2023) 135292.
[8] N.S. Yusof, S. Sapuan, M.T.H. Sultan, M. Jawaid, Life cycle analysis of hybrid oil palm/glass fibre-reinforced polyurethane composites for automotive crash box, J. Mech. Eng. Sci. 14 (2020) 7132–7140.
[9] X. Huang, Fabrication and properties of carbon fibers, Materials 2 (2009) 2369–2403.
[10] G. Chatziparaskeva, I. Papamichael, I. Voukkali, P. Loizia, G. Sourkouni, C. Argirusis, et al., End-of-Life of composite materials in the framework of the circular economy, Microplastics 1 (2022) 377–392.
[11] N. Ramawat, N. Sharma, P. Yamba, M.A.T. Sanidhi, Recycling of polymer-matrix composites used in the aerospace industry-A comprehensive review, Mater. Today: Proc. (2023). ISSN 2214-7853.
[12] Z.U. Arif, M.Y. Khalid, W. Ahmed, H. Arshad, S. Ullah, Recycling of the glass/carbon fibre reinforced polymer composites: a step towards the circular economy, Polymer-Plastics Technology and Materials 61 (2022) 761–788.
[13] M. Rani, P. Choudhary, V. Krishnan, S. Zafar, A review on recycling and reuse methods for carbon fiber/glass fiber composites waste from wind turbine blades, Compos. B Eng. 215 (2021) 108768.
[14] D. Tortorici, R. Clemente, S. Laurenzi, Solvolysis process for recycling carbon fibers from epoxy-based composites, in: 11th Conference on "Times of Polymers (TOP) & Composites, Ischia: Macromolecular Symposia, 2023.
[15] L.T. Drzal, M. Madhukar, Fibre-matrix adhesion and its relationship to composite mechanical properties, J. Mater. Sci. 28 (1993) 569–610.
[16] Z.S. Toor, Space applications of composite materials, J. Spacecraft Technol. 8 (2018) 65–70.
[17] A. Schedler, Fibre composites in satellites, Cryogenics 28 (1988) 220–223.

[18] J.-H. Han, C.-G. Kim, Low earth orbit space environment simulation and its effects on graphite/epoxy composites, Compos. Struct. 72 (2006) 218–226.
[19] E. Grossman, I. Gouzman, Space environment effects on polymers in low earth orbit, Nucl. Instrum. Methods Phys. Res. Sect. B Beam Interact. Mater. Atoms 208 (2003) 48–57.
[20] E. Toto, S. Botti, S. Laurenzi, M.G. Santonicola, UV-induced modification of PEDOT: PSS-based nanocomposite films investigated by Raman microscopy mapping, Appl. Surf. Sci. 513 (2020) 145839.
[21] M.G. Santonicola, M.G. Coscia, M. Sirilli, S. Laurenzi, Nanomaterial-based biosensors for a real-time detection of biological damage by UV light, in: 2015 37th Annual International Conference of the IEEE Engineering in Medicine and Biology Society (EMBC), IEEE, 2015, pp. 4391–4394.
[22] R.A. Kemnitz, G.R. Cobb, A.K. Singh, C.R. Hartsfield, Characterization of simulated low earth orbit space environment effects on acid-spun carbon nanotube yarns, Mater. Des. 184 (2019) 108178.
[23] P.M. Abhilash, D. Chakradhar, Image processing algorithm for detection, quantification and classification of microdefects in wire electric discharge machined precision finish cut surfaces, Journal of Micromanufacturing 5 (2022) 116–126.
[24] A.C. de Paula, F. Uliana, E.A. da Silva Filho, K. Soares, P.P. Luz, Use of DMA-material pocket to determine the glass transition temperature of nitrocellulose blends in film form, Carbohydr. Polym. 226 (2019) 115288.
[25] E. Marin, F. Boschetto, M. Zanocco, H.N. Doan, T.P.M. Sunthar, K. Kinashi, et al., UV-curing and thermal ageing of methacrylated stereo-lithographic resin, Polym. Degrad. Stabil. 185 (2021) 109503.
[26] J.W. Stansbury, M.J. Idacavage, 3D printing with polymers: Challenges among expanding options and opportunities, Dent. Mater. 32 (2016) 54–64.
[27] M. Zhang, B. Sun, B. Gu, Accelerated thermal ageing of epoxy resin and 3-D carbon fiber/epoxy braided composites, Compos. Appl. Sci. Manuf. 85 (2016) 163–171.
[28] S. Jana, W.-H. Zhong, FTIR study of ageing epoxy resin reinforced by reactive graphitic nanofibers, J. Appl. Polym. Sci. 106 (2007) 3555–3563.
[29] W. Fan, J-l Li, Y-y Zheng, T-j Liu, X. Tian, R-j Sun, Influence of thermo-oxidative aging on the thermal conductivity of carbon fiber fabric reinforced epoxy composites, Polym. Degrad. Stabil. 123 (2016) 162–169.
[30] Y. Sefrani, J.-M. Berthelot, Temperature effect on the damping properties of unidirectional glass fibre composites, Compos. B Eng. 37 (2006) 346–355.
[31] F. Aghadavoudi, H. Golestanian, Y. Tadi Beni, Investigating the effects of resin cross-linking ratio on mechanical properties of epoxy-based nanocomposites using molecular dynamics, Polym. Compos. 38 (2016).
[32] Y. Korkmaz, K. Gültekin, Effect of UV irradiation on epoxy adhesives and adhesively bonded joints reinforced with BN and B4C nanoparticles, Polym. Degrad. Stabil. 202 (2022) 110004.
[33] A. Treviso, B. Van Genechten, D. Mundo, M. Tournour, Damping in composite materials: properties and models, Compos. B Eng. 78 (2015) 144–152.
[34] A. Afaghi-Khatibi, Y.-W. Mai, Characterisation of fibre/matrix interfacial degradation under cyclic fatigue loading using dynamic mechanical analysis, Compos. Appl. Sci. Manuf. 33 (2002) 1585–1592.
[35] D.T. Burn, L.T. Harper, M. Johnson, N.A. Warrior, U. Nagel, L. Yang, et al., The usability of recycled carbon fibres in short fibre thermoplastics: interfacial properties, J. Mater. Sci. 51 (2016) 7699–7715.
[36] Y. Luo, Y. Zhao, Y. Duan, S. Du, Surface and wettability property analysis of CCF300 carbon fibers with different sizing or without sizing, Mater. Des. 32 (2011) 941–946.
[37] N. Dilsiz, J.P. Wightman, Effect of acid–base properties of unsized and sized carbon fibers on fiber/epoxy matrix adhesion, Colloids Surf. A Physicochem. Eng. Asp. 164 (2000) 325–336.
[38] Z. Dai, F. Shi, B. Zhang, M. Li, Z. Zhang, Effect of sizing on carbon fiber surface properties and fibers/epoxy interfacial adhesion, Appl. Surf. Sci. 257 (2011) 6980–6985.
[39] D. Feldman, Polymer Weathering: photo-oxidation, J. Polym. Environ. 10 (2002) 163–173.
[40] R. Talreja, J. Varna, Modeling Damage, Fatigue and Failure of Composite Materials, Elsevier, 2015.
[41] X. Yao, X. Gao, J. Jiang, C. Xu, C. Deng, J. Wang, Comparison of carbon nanotubes and graphene oxide coated carbon fiber for improving the interfacial properties of carbon fiber/epoxy composites, Compos. B Eng. 132 (2018) 170–177.
[42] Z. Shi, C. Zou, F. Zhou, J. Zhao, Analysis of the mechanical properties and damage mechanism of carbon fiber/epoxy composites under UV aging, Materials 15 (2022).
[43] A.C. Tribble, The Space Environment: Implications for Spacecraft Design-Revised and Expanded Edition, Princeton University Press, 2020.
[44] B. Banks, Spacecraft Polymers Atomic Oxygen Durability Handbook, NASA Technical Handbook, 2014.